1 **Transcriptional variability accelerates pre-leukemia by cell diversification and**

2 **perturbation of protein synthesis**

3

4 Short title: **Loss of Kat2a accelerates pre-leukemia**

5

6 One-sentence summary: **Loss of Kat2a enhances transcriptional variability of ribosome**

7 **biosynthetic programs and transiently accelerates pre-leukemia**

8

9 Shikha Gupta[1,2], Oliver M. Dovey[3#], Ana Filipa Domingues[2,4], Oliwia W. Cyran[2], Caitlin M.

10 Cash[5], George Giotopoulos[2,4], Justyna Rak[2,4], Jonathan Cooper[2,3,4], Malgorzata Gozdecka[2,4],

11 Ryan J. Asby[2,4], Noor Al-Jabery[5], Victor Hernandez-Hernandez[5,6],

12 Sudhakaran Prabakaran[1,7¶], Brian J. Huntly[2,4], George S. Vassiliou[2,3,4], Cristina Pina[5,6*]

13

14 [1]Department of Genetics, University of Cambridge, UK; [2]Department of Haematology,

15 University of Cambridge, UK; [3]Wellcome Sanger Institute, Wellcome Trust Genome

16 Campus, UK; [4]Wellcome Trust-MRC Cambridge Stem Cell Institute, University of

17 Cambridge, UK; [5]College of Health, Medicine and Life Sciences - Division of Biosciences,

18 Brunel University London, UK; [6]Centre for Genome Engineering and Maintenance, Brunel

19 University London, Uxbridge, UB8 3PH, UK; [7]NonExomics, Inc., USA *corresponding

20 author (cristina.pina@brunel.ac.uk)

21 [#]Current address: Bit.Bio; Babraham Research Campus; Cambridge, CB22 3FH; UK

22 [¶]Current address: NonExomics, Inc., 2 Simon Willard Rd, Acton, MA 01720, USA

23

24

25 Abstract: **Transcriptional variability facilitates stochastic cell diversification and can in**

26 **turn underpin adaptation to stress or injury. We hypothesize that it may analogously**

27 **facilitate progression of pre-malignancy to cancer. To investigate this, we initiated pre-**

28 **leukemia in mouse cells with enhanced transcriptional variability due to conditional**

29 **disruption of the histone lysine acetyltransferase gene *Kat2a*. By combining single-cell**

30 **RNA-sequencing of pre-leukemia with functional analysis of transformation, we show**

31 **that *Kat2a* loss results in global variegation of cell identity and accumulation of pre-**

32 **leukemic cells. Leukemia progression is subsequently facilitated by destabilization of**

33 **ribosome biogenesis and protein synthesis, which confer a transient transformation**

34 **advantage. The contribution of transcriptional variability to early cancer evolution**

35   **reflects a generic role in promoting cell fate transitions, which, in the case of well-**

36   **adapted malignancies, contrastingly differentiates and depletes cancer stem cells. In**

37   **other words, transcriptional variability confers forward momentum to cell fate systems,**

38   **with differential multi-stage impact throughout cancer evolution.**

39

40   Tumors evolve by genetic drift and natural selection [1,2]. Acquisition of new mutations confers

41   a probability of adaptation to new environmental pressures [3], and facilitates progression and

42   transformation of pre-malignant lesions, promotes metastasis and drives treatment resistance

43   [4]. In recent years, it became apparent that non-genetic instability, in particular variability in

44   methylation epialleles, can confer adaptive advantages to tumor growth and survival

45   irrespective of mutations, and function as drivers of therapy resistance and disease relapse in

46   hematological malignances [5,6]. Hematological malignances, and in particular Acute Myeloid

47   Leukemia (AML), are strongly dependent on epigenetic regulation, both through mutation of

48   chromatin factors, and by co-option of unmutated chromatin regulators into maintenance of

49   leukemogenic programs [7–9]. Notably, AML has lower levels of mutations than solid tumors,

50   supporting the notion that non-genetic events may be especially important in the former

51   [7]. Akin to genetic instability, epigenetic variability is increased in leukemia initiation and

52   relapse, but low in leukemia maintenance [10,11], suggesting that reconfiguration of

53   molecular/transcriptional programs may perturb the identity or survival of well-adapted

54   leukemia cells by disrupting pro-oncogenic molecular signatures. We have recently captured

55   this phenomenon upon loss of KAT2A, a histone acetyltransferase that promotes gene

56   transcription through activation of promoter bursting and stabilization of gene expression

57   levels. *Kat2a* loss (NULL) results in enhanced cell-to-cell transcriptional variability and

58   progressive loss of leukemia stem cells (LSC) transformed with the *KMT2A-MLLT3* (*MLL-*

59   *AF9*) gene fusion [12]. Accordingly, KAT2A is required for maintenance of AML cell lines and

60   *in vitro* self-renewal of patient AML blasts [13]. At a cellular level, loss of *Kat2a* results in

61   perturbation of leukemia lineage trajectories, with emergence of multiple incongruent

62   differentiation pathways that deplete LSC, but fail to uniformly differentiate leukemia cells

63   [12]. A similar pattern of incongruous exit from the stem cell state was observed upon KAT2A

64   inhibition in mouse embryonic stem (ES) cells [14]. MLL-AF9 results in an

65   aggressive leukemia, both in mice and in humans, and requires minimal cooperativity from

66   additional mutational events [7,15]. As such, it provides a good representation of a well-adapted

67   leukemia, with minimal genetic and epigenetic variability. However, it does not reflect what

68   is observed with more common forms of AML such as those associated with *RUNX1-*

69   *RUNX1T1* (*AML1-ETO*), where progression in mouse models is slow and infrequent [7,16], or

70   clonal hematopoiesis, in which the associated mutations (e.g. in *IDH1/2*, *TET2*, *DNMT3A*)

71   convey a self-renewal advantage, but require additional genetic events for leukemia [7,16]. In

72   these cases, we postulate that malignant progression may be facilitated by non-genetic

73   instability, which can be promoted through loss of *Kat2a*.

74

75   To test our hypothesis, we made use of 2 pre-leukemia mouse models: *Idh1^{R132H}* and *RUNX1-*

76   *RUNX1T1(RT1(9a))*. First, we developed a new inducible *Idh1^{R132H}* allele (Fig. S1a-c, and

77   Supplementary Methods), and crossed it into an *Mx1-Cre* background (Fig. S1d), to activate

78   the mutation in hematopoietic tissues. We verified the functionality of the *Idh1^{R132H}* allele by

79   accumulation of the onco-metabolite 2-HG (Fig. S1e-f). *Idh1^{R132H}* mice develop

80   leukemia rarely, with long latency and low penetrance, with no significant effects on overall

81   survival (Fig. S1g). In contrast, combination of *Idh1^{R132H}* with other leukemogenic

82   mutations, namely *NRas* and *Npm1c* (triple-mutant), results in short-latency high-penetrance

83   leukemia development (Fig. S1g), confirming the pre-leukemic nature of the *Idh1^{R132H}*

84   model. Accordingly, triple-mutant BM cells, but not cells with *Idh1^{R132H}* alone, have enhanced

85   colony-forming cell (CFC) assay replating ability, an *in vitro* measure of

86   transformation (Fig. S1h). Comparison of RNA-sequencing from triple-mutant leukemias vs

87   triple-mutant pre-leukemias, or vs *Idh1^{R132H}* alone, revealed a gene signature which was

88   specific to the leukemia state, and in which down-regulated genes were enriched

89   for *Kat2a* chromatin targets (Fig. S1i). This association suggests that loss of Kat2a activity

90   may contribute to progression of pre-leukemia to overt AML.

91

92   To investigate this putative contribution of *Kat2a* loss to pre-leukemia progression, we

93   crossed conditional *Idh1^{R132H}* and *Kat2a$^{Flox/Flox}$* mice, into the Mx1-Cre background (Fig.1a), to

94   generate *Idh1^{R132H}* animals that were heterozygous (HET) or NULL for *Kat2a* (Fig. S2a-

95   b). We analyzed *Idh1^{R132H} Kat2a$^{Flox/WT}$* (*Idh^{mut} Kat2aHET*) and

96   *Idh1^{R132H} Kat2a$^{Flox/Flox}$* (*Idh^{mut}Kat2aNULL*) animals 4 and 20 weeks after Cre induction, to

97   identify early and progressed *Idh1^{R132H}* pre-leukemia states. Analysis of BM stem and

98   progenitor composition revealed no differences between genotypes or timepoints (Fig.S2c-

99   g). We did not observe differences in spleen or liver pre-leukemia burden (Fig.S2h-

100   i). However, *Idh^{mut} Kat2aNULL* samples had a significant advantage in CFC re-plating in

101   early pre-leukemia (4 weeks) (Fig.1b), which was not sustained at the 20-week timepoint.

Fig 1
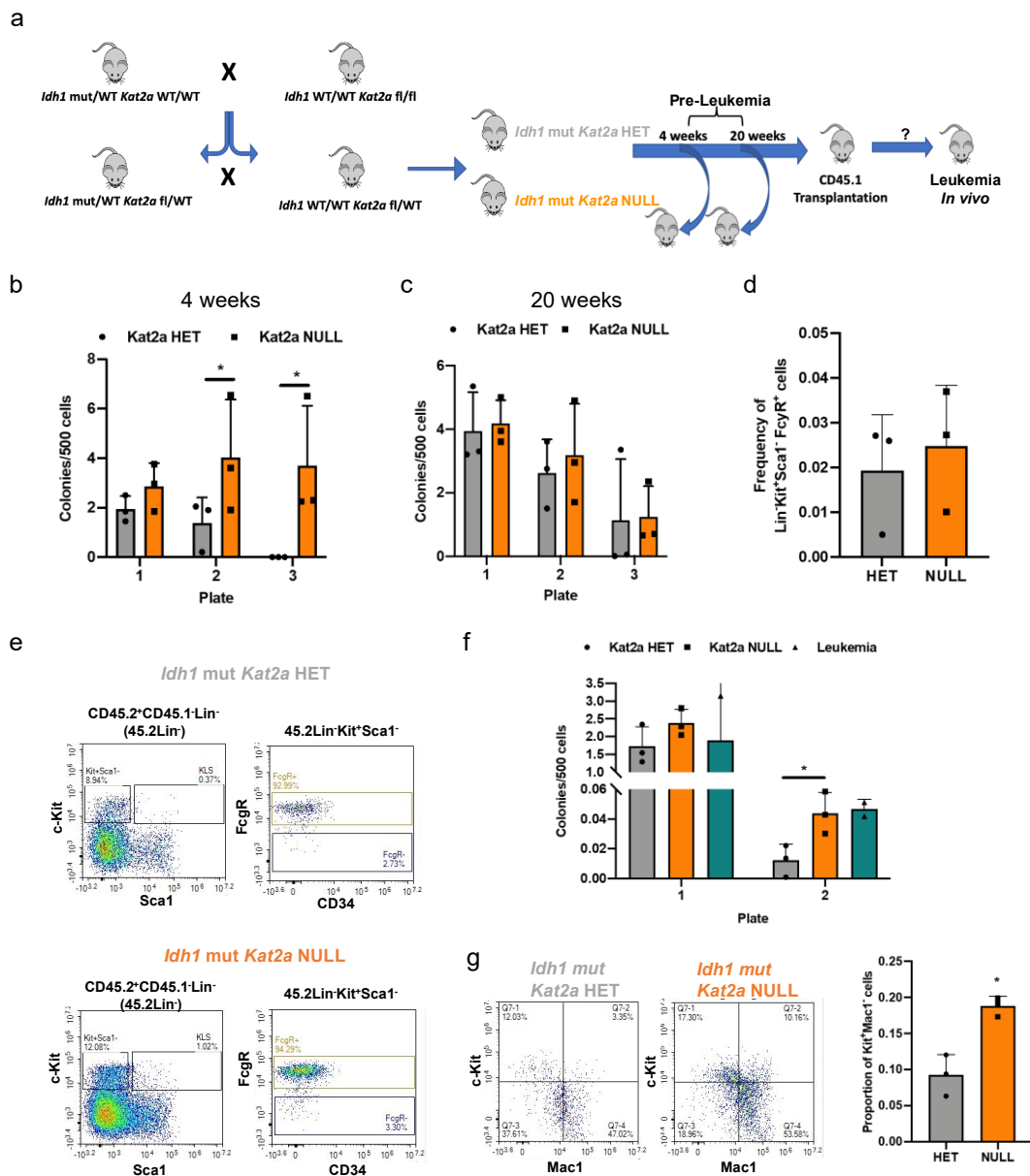
Fig. 1: *Kat2a* loss facilitates development of *Idh1^{R132H}* pre-leukemia. (A) Diagram of *Idh1^{R132H}* (*Idh1* mut) and *Kat2a* ^{fl/fl} mouse crosses to generate *Idh1* mut *Kat2a* HET and *Idh1* mut *Kat2a* NULL cells used in pre-leukemia studies. **(B)** Colony-forming cell (CFC) assays of *Idh1* mut *Kat2a* HET and NULL BM cells 4 weeks post-pIpC treatment; mean ± SD, n=3. **(C)** Colony-forming cell (CFC) assays of *Idh1* mut *Kat2a* HET and NULL BM cells 20 weeks post-pIpC treatment; mean ± SD, n=3. **(D)** Quantification of GMP-like BM cells obtained from *Idh1* mut CD45.2^+ grafts; mean ± SD, n=3 irradiated recipients (CD45.1). **(E)** Representative flow cytometry plots of BM cells in (D); top: *Idh1* mut *Kat2a* HET, bottom: *Idh1* mut *Kat2a* NULL. **(F)** Serial re-plating CFC assays of *Idh1* mut BM grafts. Mean ± SD, n=3 *Idh1* mut *Kat2a* HET and NULL, n=2 *Idh1* mut leukemia. **(G)** Flow cytometry of colonies in (F), Left, representative plots; right, Kit^+ Mac1^- progenitor quantification. Mean ± SD, n=3. All analyses 2-tailed t-test; significant *p<0.05.

114   This could be compatible with earlier selection of pre-leukemia cells upon *Kat2a* loss, which

115   is achieved later in *Idh^{mut} Kat2aHET* animals as the *Idh1^{mut}* phenotype progresses (Fig. 1c).

116   In an attempt to understand whether the early replating advantage *in vitro* could lead to

117   accelerated leukemia development *in vivo* in the absence of other genetic events, we

118   transplanted BM cells from *Idh^{mut} Kat2aHET* and *Idh^{mut} Kat2aNULL* mice, into irradiated

119   CD45.1 recipients and followed them up for 1 year. Similar to single *Idh1^{mut}* animals, we

120   could not detect signs of leukemia development in transplanted mice (Fig. S3a). Transplants

121   showed accumulation of GMP-like (Lin-Kit$^+$Sca1$^-$FcγR$^+$) donor cells, compatible

122   with myeloproliferation (Fig. 1d-e), which was identical between genotypes. Peripheral blood

123   counts (Fig.S3b-d) and spleen and liver weights (Fig.S3e-f) were also similar. However, we

124   observed infiltration of spleen and liver in 1 of 3 *Idh^{mut} Kat2aNULL* recipients, which was

125   not present in *Idh^{mut} Kat2aHET* grafts (Fig.S3g). Notably, *Idh^{mut} Kat2aNULL* cells showed

126   enhanced colony-replating potential relative to *Idh^{mut} Kat2aHET*, which was comparable to

127   that of BM from rare *Idh^{mut}* leukemic animals (Fig. 1f). *Idh^{mut} Kat2aNULL* cells in CFC

128   assays were enriched in c-Kit$^+$Mac1$^-$ cells (Fig. 1g) compatible with hindered differentiation

129   and/or expansion of self-renewing cells. Overall, the results suggest that loss

130   of *Kat2a* imparts leukemogenic properties to *Idh1^{mut}* cells but is in itself not sufficient to

131   drive leukemogenesis in the absence of additional cooperating genetic events.

132

133   We next tested the impact of *Kat2a* loss on the pre-leukemia model driven by the exon 9a

134   splicing variant of the *RUNX1-RUNX1T1* (*RT1(9a)*) fusion gene, which when retrovirally-

135   delivered to adult BM cells, leads to long-latency, incomplete-penetrance leukemia in

136   irradiated recipients. Using our previously described *Kat2a^{Flox/Flox} Mx1-Cre* mice, we

137   isolated progenitor-enriched BM cells after *pIpC*-induced locus excision (Fig. S4a),

138   and delivered the RT1(9a) construct by retroviral transduction, as described [17]. In all

139   experiments, *Kat2a^{Flox/Flox} Mx1-Cre^{+/-}* (*Kat2aNULL*) were compared with *Kat2a^{Flox/Flox} Mx1-*

140   *Cre^{-/-}* (*Kat2aWT*) cells. We started by evaluating leukemia development after

141   transplantation of RT1(9a) *Kat2aNULL* and *Kat2aWT* BM cells (Fig. 2a). Loss of *Kat2a* led

142   to a dramatic decrease in survival of RT1(9a) recipient animals, compatible with accelerated

143   leukemia progression (Fig. 2b). *Kat2a NULL* leukemias had a non-significant trend towards

144   higher white blood cell counts (Fig. S4b-d) and spleen leukemia burden, with

145   minimal infiltration of other organs (Fig. S4e-g). The surface phenotype of the

146   leukemias was indistinguishable between genotypes (Fig. S4h). Analysis of early timepoints

147   post-transplantation showed that RT1(9a) engraftment became quickly fixed in the absence

Fig 2
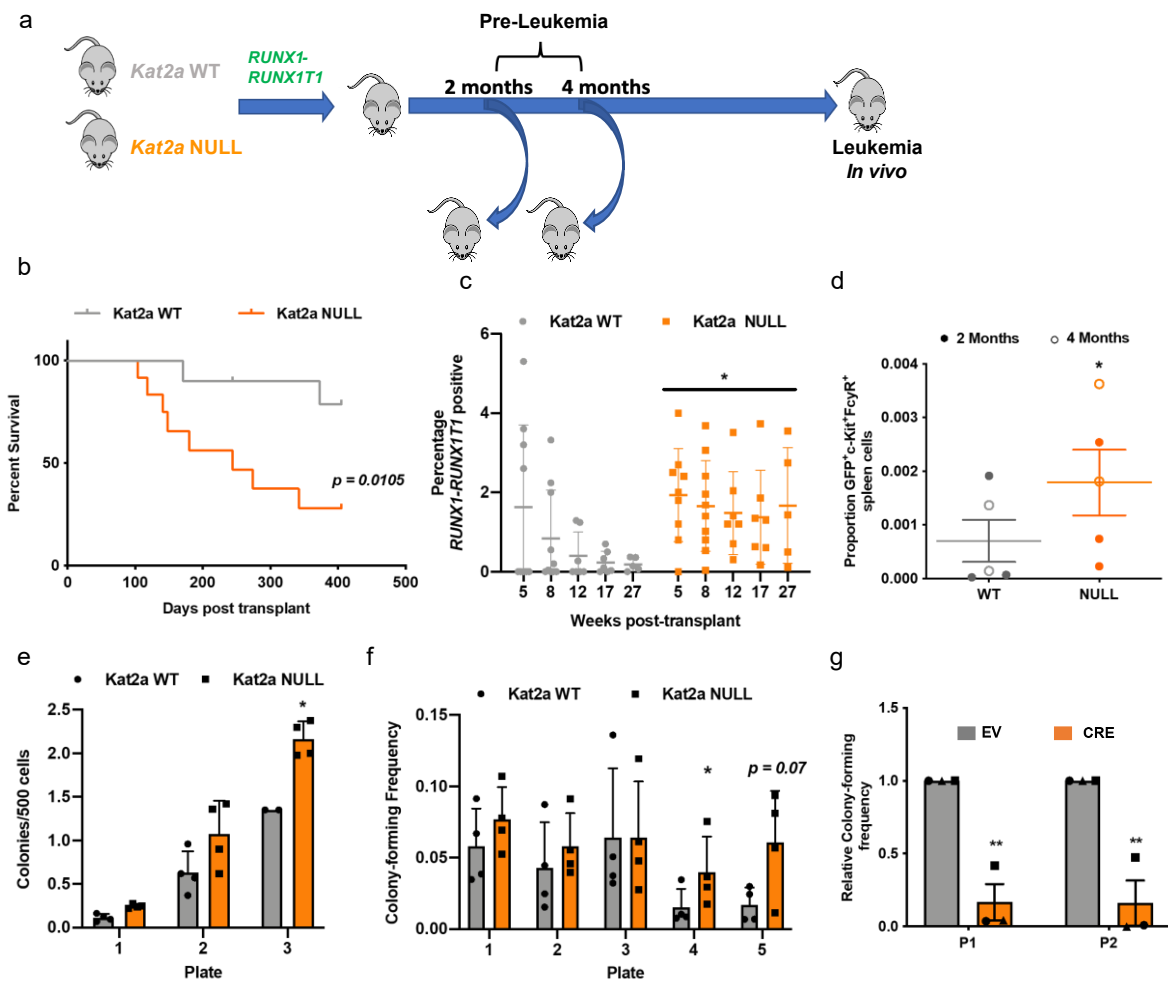
148

149 **Fig. 2: *Kat2a* loss accelerates *RT1(9a)* pre-leukemia to leukemia progression. (A)** Experimental design. **(B)**

150 Survival curve of *RT1(9a) Kat2aWT* and *Kat2aNULL* Kit+ BM recipients; n=12 animals/genotype, *p<0.05, log-rank

151 test. **(C)** Quantification of peripheral blood GFP for animals in (A); GFP reports *RT1(9a)*. Mean ± SD, n=10

152 animals/genotype (8 weeks), *p<0.05, 2-way ANOVA. **(D)** CFC assay of *RT1(9a) Kat2aWT* and *Kat2aNULL* graft

153 BM cells 4 months post-transplantation; mean ± SD, n=4. **(E)** Flow cytometry analysis of *RT1(9a) Kat2aWT* and

154 *Kat2aNULL* graft spleen cells 2- and 4-months post-transplantation; mean ± SD, n=5. **(F)** *In vitro* transformation of

155 *Kat2aWT* and *Kat2aNULL* Lin-/Kit+ BM cells transduced with *RT1(9a)* retrovirus tested in CFC serial re-plating;

156 mean ± SD, n=4. **(G)** CFC re-plating (plate=P1, P2) analysis of *RT1(9a) Kat2aFlox/Flox* Cre-/- Kit+/Lin- BM cells excised

157 *in vitro* by lentiviral-delivered *Cre* recombinase (vs. EV, empty vector) after 3 rounds of colony re-plating. Mean ±

158 SD, n=3. All other analyses 2-tailed t-test, *p<0.05, **p<0.01.

159

160

161 of *Kat2a* (Fig. 2c). *Kat2aNULL/RT1(9a)* cells obtained from healthy pre-

162 symptomatic recipients were enriched for GMP-like cells (Fig. 2d), and displayed enhanced

163 colony formation (Fig. 2e), compatible with accelerated pre-leukemia

164 development. Similarly, *Kat2aNULL* cells directly tested in CFC assays upon retroviral

165 transduction, displayed enhanced re-plating potential. (Fig. 2f). In contrast, excision

166 of *Kat2a* in RT1(9a) cells post-*in vitro* transformation by 3 rounds of serial-replating, led to a

167 reduction in colony formation (Fig. 2g), suggesting that *Kat2a* loss favors leukemia

168 development only at a pre-leukemia stage. These observations mirror our previously

169 identified role for *Kat2a* in maintenance of established leukemia stem-like cells and suggest

170 that *Kat2a* plays stage-specific roles during leukemogenesis, which are preserved across

171 leukemia models.

172

173 We had previously associated *Kat2a* function in leukemia stem cell maintenance with

174 stability of transcriptional programs [12]. Using single-cell RNA-sequencing (scRNA-seq), we

175 showed that *Kat2a* loss resulted in diversification and branching of differentiation

176 trajectories, and associated with enhanced transcriptional noise, particularly in

177 biosynthetic programs (e.g., ribosomal biogenesis and translation). We asked if similar

178 mechanisms were at play in pre-leukemia progression facilitated by *Kat2a* loss. We

179 hypothesized that enhanced transcriptional variability leading to program

180 diversification might increase the probability of accessing or seeding leukemia

181 programs, resulting in the observed acceleration in leukemia

182 progression. We performed scRNA-seq analysis of pre-leukemia cells on the 10X platform,

183 comparing transcriptional landscapes of *Kat2a*NULL and *Kat2a*WT RT1(9a) asymptomatic

184 animals obtained 2 and 4 month post-transplantation. We sequenced a total of 1767 cells

185 sorted as RT1(9a)/GFP$^+$ Kit$^+$ stem/progenitor and retrieved an average of 174770 aligned

186 reads per cell, corresponding to medians of 5939 Unique Molecular Identifiers (UMI) and

187 1575 genes per cell (Supplementary File 1). Less than 0.2% of reads aligned to mitochondrial

188 DNA, denoting successful sequencing. Pre-processing steps are detailed in Supplementary

189 Methods.

190

191 We employed transcripts of cell surface markers routinely used for hematopoietic cell

192 immunophenotyping to map the identity of cells along the pseudo-temporal trajectories

193 (Fig. S5a-b). Cells at the origin of the trajectory expressed high *Ly6e* (*Sca1*), *Cd34* and *Flt3*,

194 compatible with lymphoid-myeloid-primed progenitors (LMPP). LMPPs were adjacent to

195 a granulocyte-monocyte progenitor (GMP)-like state (*Ly6e*^{low}*Cd34*$^+$*Fcgr3*$^+$). Trajectories

196 involved 3 additional states: *Ly6e*$^+$ *CD79a*$^+$ *Cd14*$^-$ B-cell affiliated Progenitor (BAP)

197 (Supplementary File 3), and *Ly6e*$^+$*Fcgr3*$^+$*Cd14*$^+$ Monocyte-affiliated Progenitor (MAP)

Fig 3

198

199
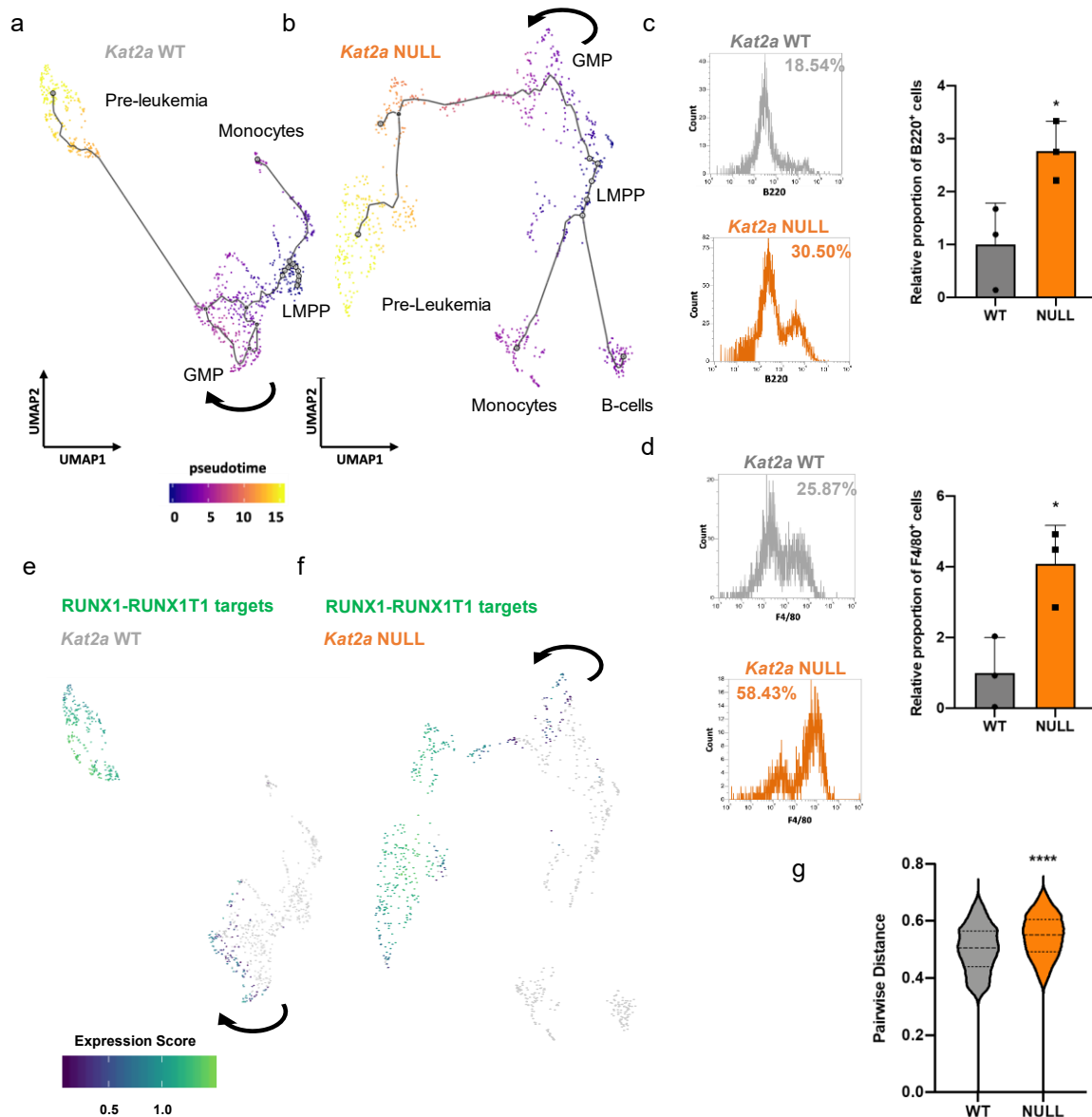
Fig. 3: Loss of *Kat2a* diversifies cell fates and promotes RT1(9a) pre-leukemia progression. (A-B) Pseudotime single-cell trajectory of **(A)** *Kat2aWT* cells, **(B)** *Kat2aNULL* RT1(9a) cells 2 and 4 months after transplantation. Trajectories inferred using Monocle3 [21]; compartments labelled as per hematopoietic markers in Fig. S5A- B. Arrows denote pseudotime progression. **(C)** B220 B-cell marker in plate 2 CFC of RT1(9a)-transduced *Kat2aWT* and *Kat2aNULL* cells during *in vitro* transformation; mean ± SD, n=3. **(D)** F4/80 monocyte marker in plate 2 CFC of RT1(9a)-transduced *Kat2aWT* and *Kat2aNULL* cells during *in vitro* transformation; mean ± SD, n=3. **(E-F)** Expression of *RUNX1-RUNX1T1* ChIP-seq targets [18] in **(E)** *Kat2aWT* cells and **(F)** *Kat2aNULL* RT1(9a) single-cell trajectories. Arrows as in A-B. **(G)** Pairwise distance transcriptional variability measure[19] of *Kat2aWT* and *Kat2aNULL* RT1(9a) cells; top 500 most variable genes/genotype calculated by distance to the median CV (DM); ****p-adj<0.0001. All analyses 2-tailed t-test, *p<0.05.

210   (Supplementary File 4), confirmed by gene ontology (GO) analysis (Fig. S5c-d); and a third

211   compartment in direct proximity of the GMP, characterized as $Ly6e^+Fcgr3^+Cd33^+Cd14^+$,

212   with no$Cd34$ or $Cd48$. BAP was exclusive to $Kat2a$NULL samples, while MAP was

213   common to both genotypes, albeit enriched in $Kat2a$NULL samples (Fig. S5e). We

214   confirmed enhanced phenotypic differentiation of $Kat2a$NULL RT1(9a) cells to the B (Fig.

215   3c) and macrophage (Fig. 3d) lineages *in vitro*. Using a signature of RT1 chromatin targets [18],

216   we identified the third compartment as the candidate pre-leukemia progenitor (PLP)

217   population (Fig. 3e-f). PLPs form a discrete (Fig. 3e) and relatively smaller

218   (Fig. S5e) compartment in the $Kat2a$WT trajectory; in contrast, the GMP-to-PLP transition

219   is more densely populated in $Kat2a$NULL pre-leukemia (Fig. 3f), with PLP comprising a

220   larger number of NULL cells. (Fig. S5e). Overall, the pseudo-temporal trajectories support

221   the notion of increased cell diversification through $Kat2a$ loss, with additional cell states

222   (BAP) and, importantly, increased size of the PLP compartment. Comparative analyses of 2

223   and 4-month pre-leukemia samples confirm the pseudo-temporal trajectory

224   findings: $Kat2a$WT RT1(9a) cells progressively differentiate from LMPP to GMP-like

225   cells (Fig. S5f) and accumulate PLPs. Pre-leukemia progression is accelerated

226   in $Kat2a$NULL RT1(9a) (Fig. S5f), which contain nearly 50% of PLPs at 4 months,

227   and uniquely display 27% of BAP cells at 2 months (Fig. S5f). The increased diversification

228   of cell types in $Kat2a$ NULL samples translated in enhanced cell-to-cell transcriptional

229   variability, measured by pairwise distance [19] (Fig. 3g, S6a). $Kat2a$NULL transcriptional

230   programs were also more variable within individual cell sub-populations (Fig. S6b),

231   indicating that the variability is likely to at least in part reflect transcriptional noise, rather

232   than differences in cellular composition alone. Comparison of transcriptional

233   variability between $Kat2a$ WT and NULL cell subpopulations shows that the GMP to PLP

234   transition itself is accompanied by enhanced transcriptional variability (Fig. S6b), supporting

235   the notion that $Kat2a$ loss may accelerate pre-leukemia progression through enhanced

236   transcriptional noise.

237

238   In order to understand the nature of the transcriptional programs perturbed upon (1) $Kat2a$

239   loss, and (2) pre-leukemia progression, we performed differential gene expression analysis of

240   the scRNA-seq dataset. Comparison of $Kat2a$NULL to WT cells revealed minimal changes in

241   gene expression levels (Fig. S7a), which were of down-regulation, as previously observed

242   upon $Kat2a$ loss [12]. Consistent with our published data [12], differentially-expressed genes

243   between genotypes predominantly associated with ribosomal assembly and translation

244
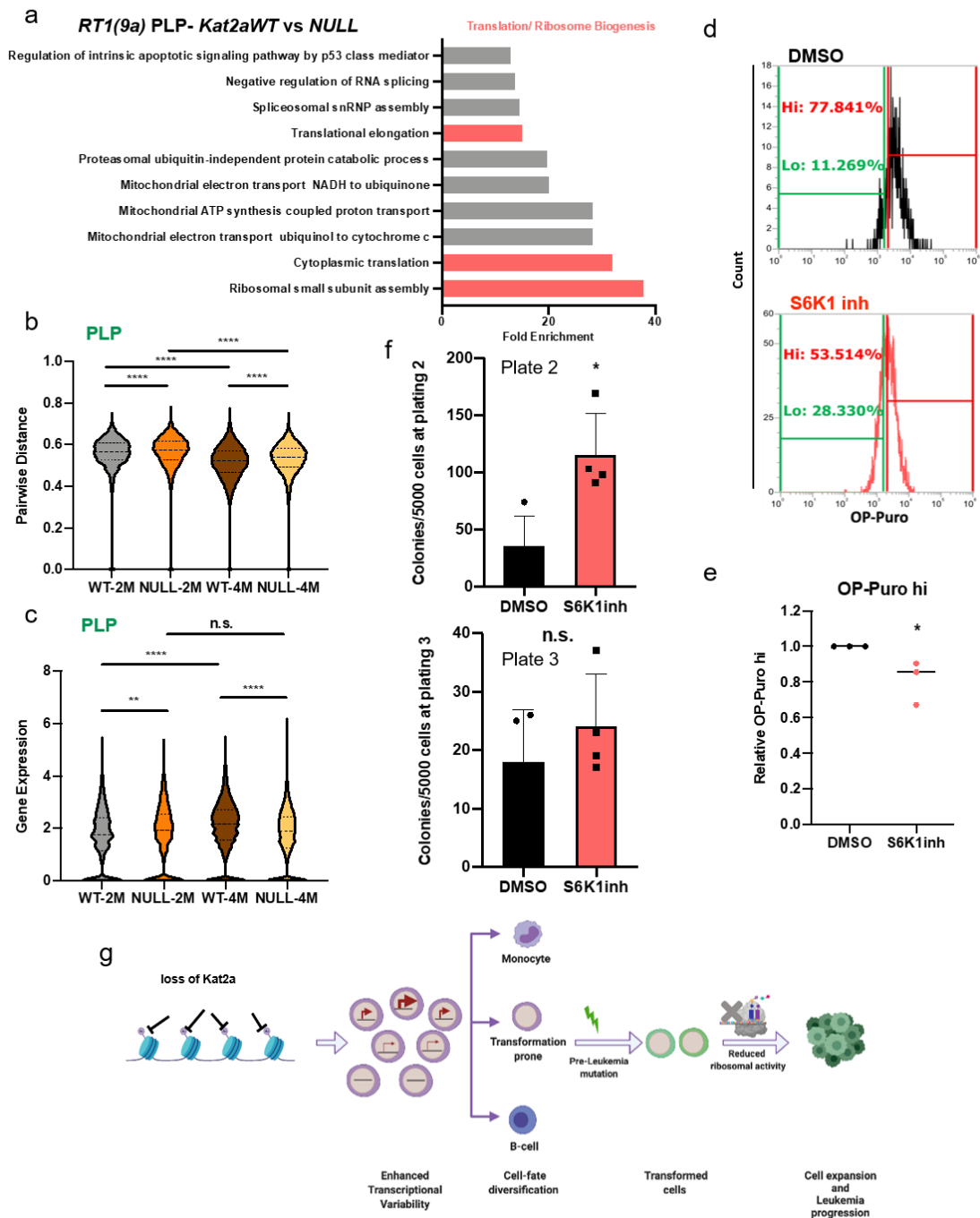
Fig. 4: Inhibition of protein synthesis phenocopies effects of *Kat2a* loss facilitating pre-leukemia

transformation. (A) Over-represented gene ontology categories (GO) for genes downregulated in RT1(9a)

Kat2aNULL vs. *WT* PLP; *p-adj<0.05. **(B)** Pairwise distance [19] of RT1(9a) PLPs; comparisons consider correlations

between ribosomal biogenesis genes ****p-adj<0.0001, 2-tailed t-test. **(C)** Distribution of expression levels for gene

signatures in (B) ****p-adj<0.0001, 2-tailed t-test. **(D)** Representative OP-Puro incorporation flow cytometry of

S6K1inh-treated RT1(9a) *Kat2aWT* cells. **(E)** Quantification of OP-Puro high cells in (E), relative to DMSO; mean ±

SD, n=3, *p<0.05, 2-tailed t-test. **(F)** CFC replating of *Kat2aWT* RT1(9a) *in vitro* transformation in the presence of

S6K1inh (control, DMSO). Plate 2 (left); mean ± SD, n=4, *p<0.05. Plate 3 (right); mean ± SD, n=4, n.s; 2-tailed t-

test. **(G)** Proposed mode of action of *Kat2a* loss in pre-leukemia progression.

254   ontologies (Fig. S7b) (Supplementary File 5), a pattern particularly prominent within

255   PLP (Fig. 4a) (Supplementary File 6). The same ontologies were specifically down-

256   regulated in *Kat2a*WT RT1(9a) PLPs compared to other cell states (Fig. S7c) (Supplementary

257   File 7), capturing a reported decrease in protein synthesis in RT1 leukemia [20]. Ribosomal and

258   translation ontologies (Fig. S7d-e) (Supplementary File 8) were also down-regulated

259   in *Idh1*[R132H] mice upon pre-leukemia-to-AML progression through additional genetic

260   mutations. Altogether, our findings suggest a specific association of attenuated ribosomal

261   programs with pre-leukemia progression, which may be further facilitated

262   by *Kat2a* loss. *Kat2a* loss increases variability of ribosomal biogenesis programs in PLPs

263   (Fig. 4b), themselves more variable than GMPs (Fig. S7f), suggesting enhanced noise at the

264   transition (Supplementary File 9). The gene expression range in *Kat2a*NULL PLPs favors

265   lower mean values (Fig. 4c). In support of the functional impact of the transcriptional

266   perturbation, *Kat2a* loss results in decreased protein synthesis (Fig. S8a-b; also [12]).

267

268   We tested the contribution of reduced protein synthesis activity to pre-leukemia progression

269   by treatment with the S6K1 inhibitor (S6K1inh) PF4708671 (Fig. S8c), which impairs

270   protein synthesis activity confirmed by reduced OP-Puro incorporation in nascent peptide

271   chains (Fig. 4d-e). We treated *Kat2a*WT RT1(9a) cells with S6K1inh and tested their

272   leukemia transformation potential *in vitro* through CFC assay re-plating. S6K1-inhibited

273   cells displayed enhanced colony-formation upon re-plating (Fig. 4f), suggesting a

274   contribution to leukemia transformation. However, the increase in colony formation was

275   transient and eventually lost upon subsequent re-plating (Fig. 4f). This suggests

276   that the effects of reduced protein synthesis on leukemia cells may vary with progression of

277   transformation, reconciling our data with prior analysis of established *MLL-AF9* cells, in

278   which reduced OP-Puro incorporation associated with *Kat2a*NULL-mediated extinction of

279   leukemia stem cells [12]. We observed a similar pattern of transient increase in colony

280   formation of *Idh1*[R132H] pre-leukemia cells treated with S6K1inh (Fig. S8d). Altogether, the

281   data suggest that reduced ribosomal assembly and protein synthesis facilitate pre-leukemia

282   progression. Exploration of lower levels of expression of translation-associated genes as a

283   consequence of enhanced transcriptional variability may be instrumental in the acceleration

284   of pre-leukemia to AML transition upon *Kat2a* loss. As leukemia progresses, variability in

285   ribosomal biosynthesis programs, may become attenuated with deviation from an optimal

286   level no longer favorable to transformation.

287

288   In this report, we have shown that *Kat2a* loss facilitates pre-leukemia progression

289   in *Idh1^{R132H}* and *RUNX1-RUNX1T1(9a)* mouse models of human disease, with acceleration of

290   frank leukemia onset in the case of RT1(9a). Loss of *Kat2a* resulted in enhanced variability

291   of transcription, leading to diversification of cell fates, including accumulation of pre-

292   leukemia progenitor cells. In the context of an early genetic event such

293   as *RT1(9a)* or *Idh1^{R132H}*, which do not allow for full leukemia transformation, the cellular

294   heterogeneity that ensues creates the opportunity for specification and expansion of

295   transformation-prone cells, on which additional molecular events may act to progress the

296   leukemic process (Fig. 4g). Amongst these, we show that destabilization of translation, which

297   is specifically targeted by *Kat2a*, acts to facilitate transformation. This may be achieved by

298   surveying and selection of biosynthetically quiescent cell states, which evade further

299   diversification and respond to additional mutations with disease propagation and progression.

300   Fully transformed, well-adapted leukemia cells may buffer transcriptional variability to

301   maintain stable self-renewal signatures and optimal biosynthetic, translation rates. In this

302   context, instability of transcriptional programs may shift biosynthetic homeostasis and

303   perturb cellular identity, and mal-adapt leukemia stem-like cells, with anti-leukemia effects.

304   Thus, stage-specific tuning and untuning of transcription and translation may be employed to

305   modulate cancer progression, a principle that can be extended to other cancer state transitions

306   such as metastasis or drug-resistance with prognostic and therapeutic potential.

307

322   Data analysis and interpretation – SG, OD, AFD, OC, CC, GSV, CP; Critical reagents – SP,

323   BJH; Writing – SG, CP, with contributions from OD, GSV. All Authors approved the final

324   version of the manuscript.

325   The Authors would like to thank: Central Biomedical Services of the University of

326   Cambridge for expert animal husbandry, CRUK Genomics Core Facility at the Cambridge

327   Research Institute, and the Wellcome Trust Sanger Research Institute Genomics Core

328   Facility for library preparation and next-generation sequencing; the Flow Cytometry facilities

329   at the Cambridge Institute for Medical Research, the NIHR Cambridge BRC Cell

330   Phenotyping Hub, and the Department of Pathology of the University of Cambridge (Dr

331   Joana Cerveira) for cell sorting; Dr Roberto Bandiera for helpful discussions and reagent

332   sharing; and Dr Matt Wayland for assistance with Cell Ranger installation and 10X

333   Genomics data matrix generation.

334   **COMPETING INTERESTS:** VH-H is co-Founder and CSO of Axovia Therapeutics. SP is

335   the CEO of NonExomics, Inc. Axovia and NonExomics did not provide funding to this study,

336   and did not influence study design, execution, data analysis or interpretation.

337   **DATA AVAILABILITY:** Single-cell RNA sequencing and bulk RNA-sequencing data were

338   deposited in ArrayExpress with accession number E-MTAB-10853 and ERP006862

339   respectively.

340

341   **SUPPLEMENTARY MATERIALS**

342   Materials and Methods

343   Table S1-S3

344   Fig S1-S8

345   References 26-32

346   Supplementary Files S1-S9

347

348   **REFERENCES**

349   1.   Greaves M, Maley CC. Clonal evolution in cancer. *Nature*. 2012;481(7381):306-313.

350   doi:10.1038/nature10762

351   2.   N M, C S. Biological and therapeutic impact of intratumor heterogeneity in cancer

352   evolution. *Cancer Cell*. 2015;27(1):15-26. doi:10.1016/J.CCELL.2014.12.001

353   3.   Zahir N, Sun R, Gallahan D, Gatenby RA, Curtis C. Characterizing the ecological and

354   evolutionary dynamics of cancer. *Nat Genet 2020 528*. 2020;52(8):759-767.

355   doi:10.1038/s41588-020-0668-4

356   4.   Persi E, Wolf YI, Horn D, et al. Mutation–selection balance and compensatory

357   mechanisms in tumour evolution. *Nat Rev Genet 2020 224*. 2020;22(4):251-262.

358   doi:10.1038/s41576-020-00299-4

359   5.   Landau DA, Clement K, Ziller MJ, et al. Locally Disordered Methylation Forms the

360   Basis of Intratumor Methylome Variation in Chronic Lymphocytic Leukemia. *Cancer*

361   *Cell*. 2014;26(6):813-825. doi:10.1016/j.ccell.2014.10.012

362   6.   Pan H, Jiang Y, Boi M, et al. Epigenomic evolution in diffuse large B-cell lymphomas.

363   *Nat Commun*. 2015;6. doi:10.1038/ncomms7921

364   7.   TCGA. Genomic and Epigenomic Landscapes of Adult De Novo Acute Myeloid

365   Leukemia. *N Engl J Med*. 2013;368(22):2059-2074. doi:10.1056/nejmoa1301689

366   8.   Dawson MA, Prinjha RK, Dittman A, et al. Inhibition of BET recruitment to

367   chromatin as an effective treatment for MLL-fusion leukaemia. *Nature*.

368   2011;478(7370):529. doi:10.1038/NATURE10509

369   9.   KM B, N Z, AU S, et al. MLL-rearranged leukemia is dependent on aberrant H3K79

370   methylation by DOT1L. *Cancer Cell*. 2011;20(1):66-78.

371   doi:10.1016/J.CCR.2011.06.010

372   10.   Shlush LI, Zandi S, Mitchell A, et al. Identification of pre-leukaemic haematopoietic

373   stem cells in acute leukaemia. *Nature*. 2014;506(7488):328-333.

374   doi:10.1038/nature13038

375   11.   Corces-Zimmerman MR, Hong WJ, Weissman IL, Medeiros BC, Majeti R.

376   Preleukemic mutations in human acute myeloid leukemia affect epigenetic regulators

377   and persist in remission. *Proc Natl Acad Sci U S A*. 2014;111(7):2548-2553.

378   doi:10.1073/pnas.1324297111

379   12.   Domingues AF, Kulkarni R, Giotopoulos G, et al. Loss of KAT2A enhances

380   transcriptional noise and depletes acute myeloid leukemia stem-like cells. *Elife*.

381   2020;9. doi:10.7554/eLife.51754

382   13.   Tzelepis K, Koike-Yusa H, De Braekeleer E, et al. A CRISPR Dropout Screen

383   Identifies Genetic Vulnerabilities and Therapeutic Targets in Acute Myeloid

384   Leukemia. *Cell Rep*. 2016;17(4):1193-1205. doi:10.1016/j.celrep.2016.09.079

385   14.   Moris N, Edri S, Seyres D, et al. Histone Acetyltransferase KAT2A Stabilizes

386   Pluripotency with Control of Transcriptional Heterogeneity. *Stem Cells*.

387   2018;36(12):1828-1838. doi:10.1002/stem.2919

388   15.   Somervaille TCP, Cleary ML. Identification and characterization of leukemia stem

389   cells in murine MLL-AF9 acute myeloid leukemia. *Cancer Cell*. 2006;10(4):257-268.

390   doi:10.1016/j.ccr.2006.08.020

391 16. Papaemmanuil E, Gerstung M, Bullinger L, et al. Genomic Classification and

392   Prognosis in Acute Myeloid Leukemia. *N Engl J Med*. 2016;374(23):2209.

393   doi:10.1056/NEJMOA1516192

394 17. Basheer F, Giotopoulos G, Meduri E, et al. Contrasting requirements during disease

395   evolution identify EZH2 as a therapeutic target in AML. *J Exp Med*. 2019;216(4):966-

396   981. doi:10.1084/jem.20181276

397 18. Ptasinska A, Assi SA, Mannari D, et al. Depletion of RUNX1/ETO in t(8;21) AML

398   cells leads to genome-wide changes in chromatin structure and transcription factor

399   binding. *Leukemia*. 2012;26(8):1829-1841. doi:10.1038/leu.2012.49

400 19. Mohammed H, Hernando-Herraez I, Savino A, Nichols J, Marioni JC, Correspondence

401   WR. Single-Cell Landscape of Transcriptional Heterogeneity and Cell Fate Decisions

402   during Mouse Early Gastrulation. *CellReports*. 2017;20:1215-1228.

403   doi:10.1016/j.celrep.2017.07.009

404 20. Cai X, Gao L, Teng L, et al. Runx1 Deficiency Decreases Ribosome Biogenesis and

405   Confers Stress Resistance to Hematopoietic Stem and Progenitor Cells. *Cell Stem Cell*.

406   2015;17(2):165-177. doi:10.1016/j.stem.2015.06.002

407 21. Trapnell C, Cacchiarelli D, Grimsby J, et al. The dynamics and regulators of cell fate

408   decisions are revealed by pseudotemporal ordering of single cells. *Nat Biotechnol*.

409   2014;32(4):381-386. doi:10.1038/nbt.2859

410 22. WC S, B R, AP W, et al. A conditional knockout resource for the genome-wide study

411   of mouse gene function. *Nature*. 2011;474(7351):337-344.

412   doi:10.1038/NATURE10163

413 23. Rodríguez CI, Buchholz F, Galloway J, et al. High-efficiency deleter mice show that

414   FLPe is an alternative to Cre-loxP. *Nat Genet 2000 252*. 2000;25(2):139-140.

415   doi:10.1038/75973

416 24. Dovey OM, Cooper JL, Mupo A, et al. Molecular synergy underlies the co-occurrence

417   patterns and phenotype of NPM1-mutant acute myeloid leukemia. *Blood*.

418   2017;130(17):1911-1922. doi:10.1182/BLOOD-2017-01-760595

419 25. Basheer F, Giotopoulos G, Meduri E, et al. Contrasting requirements during disease

420   evolution identify EZH2 as a therapeutic target in AML. *J Exp Med*. 2019;216(4):966-

421   981. doi:10.1084/jem.20181276

422